Metastable Phase Formation from Nd-Dy-Fe-B Undercooled Melt

Shumpei OZAWA[1], Akira ITOU[2] , Kazuhiko KURIBAYASHI[3],
Noriyuki NOZAWA[4], and Satoshi HIROSAWA[5]

[1] Department of Aerospace Engineering, Tokyo Metropolitan University, Tokyo, Japan, shumpei.ozawa@tmu.ac.jp
[2] Graduate school of Tokyo Metropolitan University, Tokyo, Japan, akira.itou@isas.jaxa.jp
[3] Institute of Space and Astronautical Science, Japan Aerospace Exploration Agency, Sagamihara, Japan, kuribayashi@isas.jaxa.jp
[4] Magnetic Materials Research Laboratory, NEOMAX Company, Hitachi Metals, Ltd., Mishima, Japan, noriyuki_nozawa@hitachi-metals.co.jp
[5] Magnetic Materials Research Laboratory, NEOMAX Company, Hitachi Metals, Ltd., Mishima, Japan, sahoshi_hirosawa@hitachi-metals.co.jp

Abstract

$Nd_{10-x}Dy_xFe_{85}B_5$ (x = 0-3) alloy samples were melted and then solidified in the containerless state of a drop tube at oxygen partial pressure of 10^{-1}Pa. The calculated cooling rate of the spherical sample was over 10^3K/s. The $Nd_{10}Fe_{85}B_5$ sample consists of the $Nd_2Fe_{17}B_x$ metastable phase together with the α-Fe dendrite. The metastable phase was partially decomposed into small grains of $Nd_2Fe_{14}B$ and α-Fe phases by a solid state decomposition reaction. The substitution of Dy for Nd in the range from 10 to 20 atomic percent was effective to suppress the primary formation of the α-Fe dendrite and to promote the formation of the $RE_2Fe_{17}B_x$ metastable phase. When the substitution rate of Dy increased to 30 atomic percent, a large amount of the α-Fe dendrite was formed because an oxide layer of rare earth elements was generated at the sample surface due to the easy oxidization tendency of Dy.

1. Introduction

Nanocomposite magnets are theoretically expected to have high maximum energy products due to an exchange interaction if nano-scale hard and soft magnetic phases are arranged in the most appropriate manner [1)]. This magnet is currently prepared by the annealing of amorphous melt-spun ribbon [2)]. In this case the volume fraction of $Nd_2Fe_{14}B$ hard magnetic phase is inevitably limited because the alloy composition of $Fe_3B/Nd_2Fe_{14}B$ which has high amorphous formability is used, resulting in a much lower coercivity of the magnet [2)]. Furthermore, the resultant nanocomposite magnets have limited shape such as powder and ribbon.

When the $Nd_xFe_{100-1.5x}B_{0.5x}$ (x = 10-14) alloys solidify from the undercooled melt using containerless processing such as an electromagnetic levitation and drop tube method, the $Nd_2Fe_{17}B_x$ metastable phase is crystallized [3-5)]. The metastable phase is decomposed into a nanosized microstructure which consists of the magnetically soft α-Fe and hard $Nd_2Fe_{14}B$ phases by a solid state decomposition reaction [4, 5)]. If this decomposed microstructure can be applied to the production of nanocomposite magnets, they could be mass produced. The volume fraction of the $Nd_2Fe_{14}B$ phase increases more than that of the practical $Nd_2Fe_{14}B/Fe_3B$ nanocomposite magnet. Moreover, the α-Fe phase whose saturation magnetization is larger than that of the Fe_3B phase acts as a soft magnetic phase [2, 6)]. Thus, the maximum energy product of the magnets is improved. These are major advantages compared with the $Nd_2Fe_{14}B/Fe_3B$ type nanocomposite magnet prepared by rapid solidification techniques.

In order to apply the decomposition of the metastable phase to the development of the nanocomposite magnets, coarse α-Fe dendrites which grow at a small undercooling level should be eliminated because it decreases the coercivity of the magnet [7, 8)]. Furthermore, the alloy size should be enlarged from the view point of productivity. Preparing the alloy to respond to the cooling rate and undercooling level simultaneously is contradictory; high cooling rate and large undercooling level of the melt are important to suppress the α-Fe dendrite though these values are decreased when the alloy size becomes large [4, 5)].

Grieb *et al*. reported that the substitution of Tb or Dy for Nd in the rapidly solidified $RE_2Fe_{14}B$ (RE = Nd + Dy or Tb) alloy expands the formation temperature range of the Nd_2Fe_{17} type metastable phase as shown in **Fig. 1** [9)]. Furthermore, the formation region of the α-Fe phase becomes narrow with an increased substitution ratio of Dy or Tb. This suggests that there is a possibility of forming the metastable phase without the α-Fe formation even at a small undercooling of the melt. Consequently, a large alloy would be produced.

In the present study, the $Nd_{10-x}Dy_xFe_{85}B_5$ (x = 0-3) alloys were solidified from the undercooled melt using drop tube processing. The relationships among the constituent phase, substitution ratio, and sample diameter were examined. The purpose of this investigation is to explore the possibility of the formation of the metastable the phase free from the α-Fe formation in a bulk alloy. Furthermore, the

thermal stability of the metastable phase was investigated.

2. Experiment

Small segments of Nd-Fe-B alloy with the nominal composition of $Nd_{10-x}Dy_xFe_{85}B_5$ (x = 0-3) were charged into a quartz crucible with an orifice from 0.1 to 0.5mm in diameter at the bottom. The quartz crucible filled with the alloy was fixed in a chamber rigged at the top of the drop tube as shown in **Fig. 2**. The free fall length of the drop tube is 26 m. The drop tube was initially evacuated to the order of 10^{-4} Pa and then backfilled with 99.999% pure He. The oxygen partial pressure of the refilled gas was less than 10^{-1} Pa. The alloy was inductively melted and superheated to temperatures approximately 100 K higher than the liquidus temperature. The temperature of the melt was monitored at the center of the crucible by a thermocouple encased in a quartz glass sheath. The molten alloy was ejected from the orifice into the drop tube by helium gas pressurized to 0.15 MPa higher than the surrounding environment. The ejected melt shaped into small droplets of various sizes which rapidly solidified during free fall. The calculated cooling rate of the sample is shown in **Fig. 3.** The detail of the calculation can be found elsewhere [10].

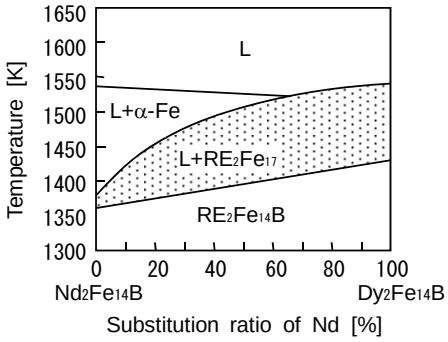

Fig. 1 Temperature – composition sections along different $RE_2Fe_{14}B$ phases as a function of substitution ratio of Dy for Nd.

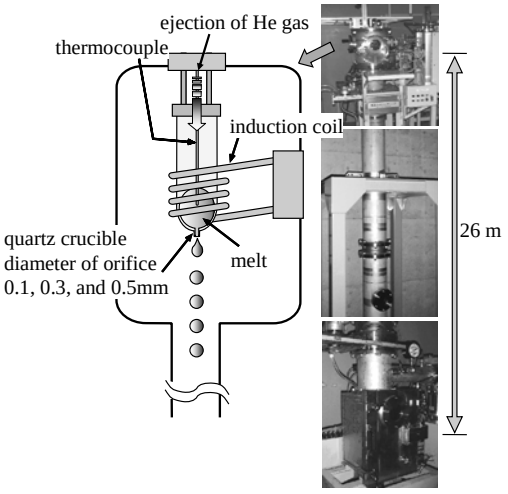

Fig. 2 Schematic of drop tube facility

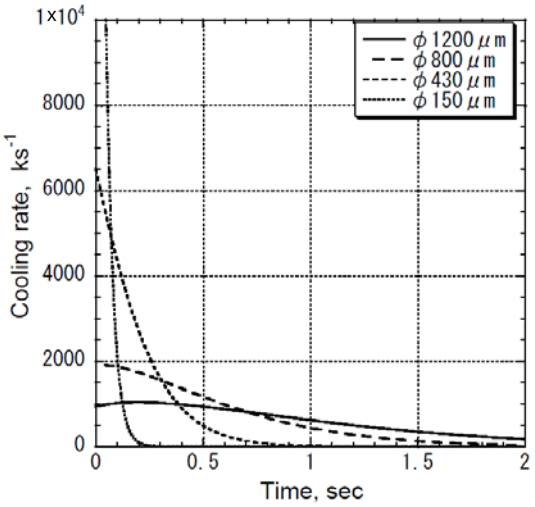

Fig. 3 Cooling rates of droplets with various diameters as a function of flight time.

The constituent phases of the as-solidified samples were identified by powder X-ray diffraction (XRD) analysis using Cu-K_α radiation at room temperature. The microstructure of the sample was examined by scanning electron microscopy (SEM) using an energy dispersive X-ray (EDX) analyzer. The accelerating voltage of EDX analysis was controlled at 10 kV. It was carried out on the surface of the cross section, which was polished only mechanically so as not to lose the details of the microstructure. The differential thermal analysis (DTA) of the sample was carried out in an argon atmosphere at a heating rate of 0.5 Ks^{-1}.

3. Results and Discussions

Fig. 4 shows the XRD profiles of the as-dropped samples. The XRD profile of the $Nd_{10}Fe_{85}B_5$ with a diameter range of 850 μm and 1200 μm indexed to the diffraction peaks of the $Nd_2Fe_{14}B$ phase, α-Fe phase and metastable $Nd_2Fe_{17}B_x$ phase.

Even when the sample diameter is comparatively large in the range of 1200 μm to 1500 μm, the diffraction peaks of the $RE_2Fe_{14}B$ phase disappear in the XRD profile of the $Nd_9Dy_1Fe_{85}B_5$ sample as shown in fig. 4 (b). Furthermore the relative intensity of the diffraction peaks of the α-Fe phase becomes half when compared with the 850 μm and 1200 μm diameter range sample of $Nd_{10}Fe_{85}B_5$, implying that the volume fraction of the α-Fe phase decreases by 50% due to the substitution of Dy for Nd. These results reveal that the substitution of Dy for Nd is effective for enhancement of the formability of the $RE_2Fe_{17}B_x$ phase and for suppressing the α-Fe formation. Almost the same XRD profile is obtained in the $Nd_8Dy_2Fe_{85}B_5$ sample.

The Fe_3RE, Fe_3B, RE, and Re_2O_3 phases are formed

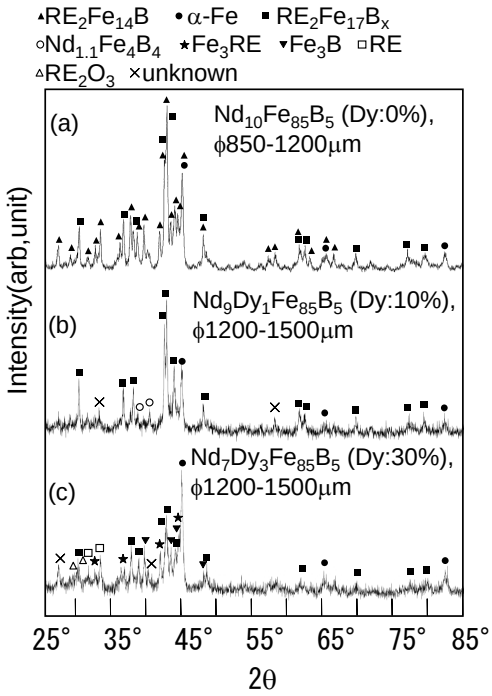

Fig. 4 XRD profiles of (a) as-dropped $Nd_{10}Fe_{85}B_5$ samples with a diameter of ϕ850 - 1200 μm, (b) $Nd_9Dy_1Fe_{85}B_5$ samples with a diameter of ϕ1200 - 1500 μm, and (c) $Nd_7Dy_3Fe_{85}B_5$ samples with a diameter of ϕ1200 – 1500 μm

when the substitution ratio of Dy for Nd is increased to 30%. As a result, the volume fraction of the metastable phase is decreased in the sample.

Fig. 5 exhibits the typical microstructures of the as-dropped samples. In the ternary $Nd_{10}Fe_{85}B_5$ samples α-Fe dendrite is embedded in the $Nd_2Fe_{17}B_x$ phase as shown in fig. 5 (a). This indicates that the γ-Fe phase, which transforms into the α-Fe phase at room temperature, was formed directly from the melt as the properitectic phase and followed by the $Nd_2Fe_{17}B_x$ phase. The $Nd_2Fe_{14}B$ phase, which fills the area between the $Nd_2Fe_{17}B_x$ phases, would be finally solidified from the remaining melt [5]. The $Nd_2Fe_{17}B_x$ metastable phase is partially transformed into the α-Fe and $Nd_2Fe_{14}B$ phases by solid state decomposition reaction.

Excluding large α-Fe dendrites the microstructure of the $Nd_9Dy_1Fe_{85}B_5$ and $Nd_8Dy_2Fe_{85}B_5$ sample with a diameter of 1200 μm to 1500 μm are almost the same as that of the $Nd_{10}Fe_{85}B_5$ with a diameter of 850 μm to 1200 μm as shown in fig. 5 (b). A part of the $RE_2Fe_{17}B_x$ phase is decomposed into the α-Fe and $RE_2Fe_{14}B$ phases as is the case of the ternary $Nd_{10}Fe_{85}B_5$, indicating that the substitution of Dy for Nd up to 20at% does not influence the decomposition of the $RE_2Fe_{17}B_x$ phase. In other words, the $RE_2Fe_{17}B_x$ phase still remains as a metastable phase even when Dy up to 20% is substituted for Nd in the $Nd_{10}Fe_{85}B_5$ alloy. Because the volume fraction of the $Nd_2Fe_{14}B$ phase is limited, no appreciable diffraction peaks for the $Nd_2Fe_{14}B$ phase would be detected in the XRD profile of $Nd_9Dy_1Fe_{85}B_5$ and $Nd_8Dy_2Fe_{85}B_5$ samples with a diameter range of 1200 μm to 1500 μm.

In the microstructure of the $Nd_7Dy_3Fe_{85}B_5$ sample with a diameter of 1200 μm to 1500 μm, a very thick layer of the RE_2O_3 phase is formed at the sample surface as exhibited in **Fig. 6**. According to the Ellingham diagram for Fe_3O_4, Fe_2O_3, Nd_2O_3, and Dy_2O_3 (cf. **Fig. 7**), the data of which are calculated from the standard entropy and standard enthalpy change of formation of those phases [11], oxidization tendency of Dy is higher than that of Nd. Therefore, a large amount of the substitution of Dy for Nd must be responsible for such a thick oxide layer in the $Nd_7Dy_3Fe_{85}B_5$ sample. Furthermore, the properitectic α-Fe dendrite would form easily due to the consumption of the rare earth elements. These results indicate that the substitution ratio of Dy for Nd should be less than 20% for preparing the alloys to develop the nanocomposite magnet using the decomposition of the $RE_2Fe_{17}B_x$ metastable phase.

As mentioned above, the substitution of Dy for Nd in the $Nd_{10}Fe_{85}B_5$ alloys up to 20% is very effective to enhance the formability of the $RE_2Fe_{17}B_x$ phase and to suppress the α-Fe formation. However, the RE elements were oxidized at the melt surface preferentially when

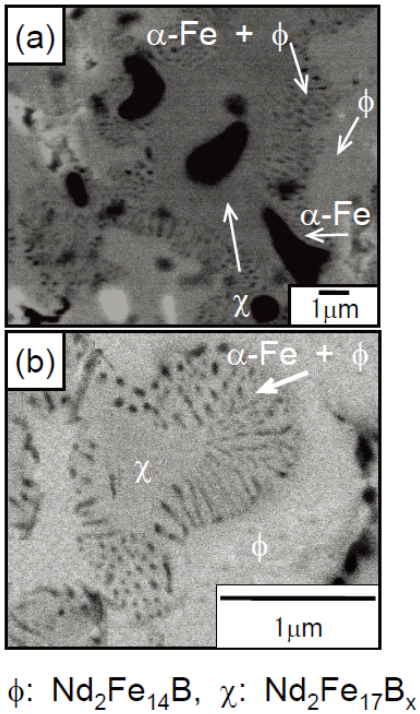

Fig. 5 Backscattered SEM micrographs of (a) as dropped $Nd_{10}Fe_{85}B_5$ samples with a diameter of ϕ850 - 1200 μm, and (b) $Nd_9Dy_1Fe_{85}B_5$ samples with a diameter of ϕ1200 - 1500 μm.

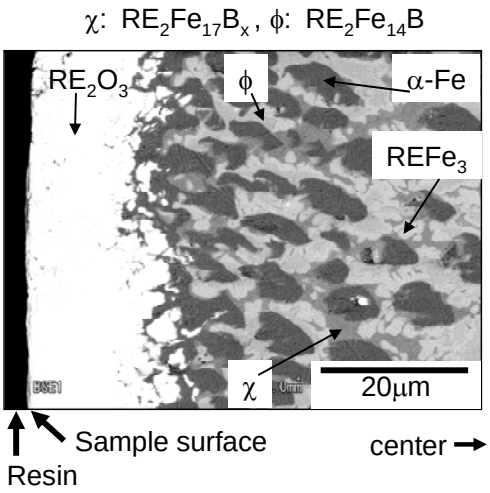

Fig.6 Backscattered SEM micrographs of $Nd_7Dy_3Fe_{85}B_5$ samples with a diameter of ϕ1200 - 1500 μm. The microstructure was observed at the edge of the cross section of the sample.

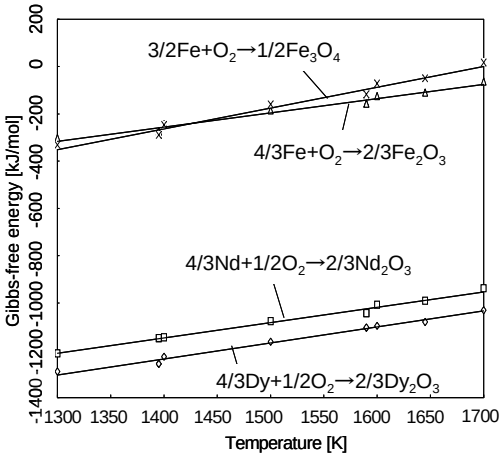

Fig. 7 Ellingham diagram for Fe_2O_3, Fe_3O_4, Nd_2O_3, and Dy_2O_3.

the substitution of Dy was 30%. According to Grieb and co-workers [9], the formation temperature range of the $RE_2Fe_{17}B_x$ phase expands and that of the α-Fe phase becomes narrow with increasing substitution of Dy for Nd (cf. figure 1). If a lower oxygen partial pressure in the drop tube is achieved, further substitution of Dy for Nd may become effective for enhancement of the formation of the metastable phase and for suppression of coarse α-Fe dendrite even at lower cooling rate and smaller undercooling level. In this case larger alloys which consist of the metastable phase free from the α-Fe dendrite can be produced.

4. Conclusions

Nd-Fe-B alloys with nominal compositions of $Nd_{10-x}Dy_xFe_{85}B_5$ (x = 0-3) were solidified in the containerless state during their free fall at oxygen partial pressure of 10^{-1}Pa. The influences of the substitution of Dy for Nd in the $Nd_{10}Fe_{85}B_5$ alloys solidified from the undercooled melt were investigated. The calculated cooling rate of the spherical sample was over 10^3K/s.

The $Nd_{10}Fe_{85}B_5$ sample with a diameter in the range of 850 μm to 1200 μm consisted of $Nd_2Fe_{17}B_x$ metastable phase and $Nd_2Fe_{14}B$ phase together with a large dendrite of the α-Fe phase. The metastable phase was partially transformed into the $Nd_2Fe_{14}B$ and α-Fe phases by solid state decomposition reaction.

Although almost the same microstructures were observed in the $Nd_9Dy_1Fe_{85}B_5$ and $Nd_8Dy_2Fe_{85}B_5$ samples, the α-Fe dendrite was not observed even when the sample diameter was 1200 μm to 1500 μm. The $RE_2Fe_{17}B_x$ metastable phase, where Nd was partially substituted by Dy, decomposed into the $RE_2Fe_{14}B$ and α-Fe phases through the solid state decomposition reaction as was the case of the ternary $Nd_2Fe_{17}B_x$ metastable phase.

When the substitution rate of Dy for Nd was increased to 30%, a thick oxide layer of the rare earth element formed at the sample surface. A huge amount of a large α-Fe dendrite was formed due to the consumption of the rare earth elements.

Acknowledgements

This work was financially supported by a grant-in-aid for Scientific Research from the Ministry of Education, Culture, Sports, Science, and Technology. Parts of this study were supported by the Iketani Science and Technology Foundation. The authors would like to thank Prof. Hibiya (System Design and Management Research Center, Keio Univ., Japan) for his helpful discussions.

References

1) Kneller, E. F. and Hawig, R., *IEEE Trans. Mag.*, **27**, 3588, 1991.
2) Coehoorn, R., DE Mooji, D.B., Duchateau, J.P.W.B., and Buschow, K.H.J., *J de Phys* **49,** C8, 1988.
3) Gao, J., Volkmann, T., and Herlach, D. M., *Acta Mater*, **50**, 3003, 2002.
4) Ozawa, S., Li, M., Sugiyama, S., Jimbo, I., Hirosawa, S., and Kuribayashi, K., *Materials Science and Engineering*, **A382**, 295, 2004.
5) Ozawa, S., Kuribayashi, K., Hirosawa, S., Reutzei, S., and Herlach, D. M., *J. appl. phys.* **100**, 1, 123906, 2006.
6) Gangopadhyay, S., Hadjipanayis, G. S., Dale, B., Sorensen, C. M., Klabunde, K. J., Paraefthymiou, V., and Kostikas, A., *Physical Review B.*, **45**, 9778, 1992.
7) Ahmed, M., Edgley, D. S., and Harris, I. R., *J. Alloys Compd.* **224**, 135, 1995.
8) Ozawa, S., Saito, T., and Motegi, T., *J. Alloys Compd.* **363**, 263, 2004
9) Grieb, B., Schneider, G., Henig, E. T., and Petzow, G., *Z.Metallkde.*, **Bd.80**, 515, 1989H. 7
10) Ozawa, S., Kuribayashi, K., and Hibiya, T., *J. Jpn. Soc. Microgravity Appl.* **24**, 9, 2007.
11) Knacke, O., Kubaschewski, O. and Hesselmann, K., ‘‘Thermodynamic Properties of Inorganic Substances 1 and 2’’, Springer-Verlag, 1991